Dissolution of precipitates heated above the solubility line: A Monte Carlo simulation

I. Žižak, P. Fratzl, and O. Penrose*
Institut für Materialphysik der Universität Wien, Boltzmanngasse 5, A-1090 Wien, Austria
(Received 10 January 1997)

The use of precipitate hardened alloys at high temperatures is often limited by the thermal stability of the precipitates. To improve the understanding of precipitate dissolution after a rapid increase of temperature, we used computer simulation to study a binary $A-5$ at. % B model alloy. The system consisted of A and B atoms on a quadratic lattice with nearest-neighbor attractive interactions between like atoms. The dynamics was provided by a single vacancy moving across the lattice by exchanges with neighboring atoms. The evolution of the precipitates was studied as a function of time at various temperatures T_a, starting from a given initial configuration, which was prepared by ''annealing'' a random mixture of A and B atoms at a low temperature inside the miscibility gap of the alloy. Depending on the new temperature T_a, different processes were observed. For T_a inside the miscibility gap, the precipitates stayed compact and dissolved partially at first, but afterwards their average size increased again by a coarsening process. For T_a outside the miscibility gap, but below the critical temperature T_c, the precipitates stayed compact and dissolved completely by evaporation of atoms from their surfaces. Above T_c, they decomposed rapidly into many smaller particles in a process that resembles an explosion. A theoretical description of these various processes, based on a phase field model, is presented. [S0163-1829(97)03018-X]

I. INTRODUCTION

The kinetics of nucleation and growth of precipitates in alloys has been very extensively studied in recent years[1,2] both because it is an interesting case of nonequlibrium thermodynamics and because it corresponds to a technologically important process whereby the hardness of an alloy may be considerably increased. The inverse process where precipitates dissolve after an increase in temperature has attracted much less attention, even though this inverse process is also very important technologically. Indeed, the fact that the precipitates may dissolve again during service of the material is often the crucial limitation for the use of precipitate-hardened alloys at high temperatures. Consequently, while knowledge about the nucleation and growth of precipitates is important for the preparation of precipitate-hardened alloys, knowledge about the dissolution processes of precipitates is equally essential for understanding their stability.

Only a small number of experiments have been carried out to study dissolution in alloy systems. In some cases, like Al-Zn,[3–5] the average precipitate radius was found to increase continuously during dissolution, whereas in other systems, like Al-Li,[6] it decreased. A tentative explanation for the increasing radius in Al-Zn has been given in terms of a Zn-rich shell surrounding the precipitates which dissolves by diffusion.[7,8]

The purpose of the present work is to get a better understanding of these phenomena by means of a computer simulation. The general principles for using simulations in such work are well understood.[1,9,10] We use an Ising model on a plane square lattice with nearest-neighbor interaction, the dynamics being provided by a single vacant site which travels through the lattice by exchanging places with the occupants of neighboring sites.[11] The alloy is first quenched to a point inside the misciblity gap of the phase diagram and left there long enough for well-defined precipitates of the minority phase to form. Then the temperature is raised to a new value and the behavior of the precipitates is studied.

We find that two quite different dissolution mechanisms can operate, depending on the final temperature. If the final temperature is below the critical temperature T_c, the precipitates stay compact and dissolve mostly by evaporation at their surfaces, eventually disappearing altogether if the final phase point is outside the misciblity gap of the phase diagram. On the other hand, if the final temperature is above T_c, the precipitates ''explode'' almost immediately into a large number of small pieces which then drift apart by diffusion. We show, using quantitative data from the simulations, how these two different mechanisms can be understood in terms of the interdiffusion of the alloy atoms and the properties of the interfaces at the boundaries of the precipitates, which continue to exist if the temperature is below T_c but disappear if it is above.

II. DESCRIPTION OF THE SIMULATION

The simulation was performed on a 512×512 square lattice, using periodic boundary conditions so as to diminish the finite-size effects. The Hamiltonian is

$$\mathcal{H}=-J\sum_{\langle i,j\rangle}\sigma_i\sigma_j. \tag{1}$$

The summation is taken over all nearest-neighbor pairs and σ_i takes the value 1, -1, or 0, if there is an A atom, a B atom, or a vacancy at site i, respectively. The positive number J is the interaction energy between neighboring sites, and determines the critical temperature:[12]

$$\frac{J}{k_BT_c}=\frac{1}{2}\ln(1+\sqrt{2}). \tag{2}$$

In this model, the vacancy does not interact directly with A or B atoms and it has no preference for the A-rich or the B-rich phase. It is, however, attracted to the interface between A-rich and B-rich phases.[11]

At each simulation step the vacancy attempts to change place with one of the neighboring atoms chosen at random. The Metropolis rule is used to determine the exchange probability

$$W=\min[1,\exp(-\Delta E/kT)], \tag{3}$$

where ΔE denotes the increase in energy if the exchange takes place.

The concentration of B atoms was taken to be 5 at.%. Two sets of simulations were made. In the first set, the simulated alloys were first quenched from infinitely high temperature and aged for 30 000 MCS (MCS = Monte Carlo steps = attempted interchanges per site) at different temperatures in and outside the miscibility gap. The purpose of these simulations was to test that the model reproduced known growth laws for the precipitates. For the second set of simulations, the alloy was first quenched from infinite temperature to $T/T_c=0.5$ where it was aged for a time of 10 000 MCS to prepare the initial configuration. Then the temperature was changed to a new (final) value and the simulation proceeded for a further 30 000 MCS. The final temperatures used for both types of runs were $T/T_c=0.5$, 0.65, 0.75, 0.85, 0.95, 1.05, 1.15, and 2.0. All the simulations were repeated five times to improve their statistical reliability.

At the chosen concentration of B atoms, $c=5\%$, the boundary of the miscibility gap T_M can be computed from Yang's formula[13] for the spontaneous magnetization m^* of the Ising ferromagnet,

$$m^*=[1-(\sinh 2J/kT)^{-4}]^{1/8}, \tag{4}$$

to be $T_M/T_c=0.8954$. It follows (see Fig. 5) that the phase points with $T/T_c=0.5$–0.85 are all inside the miscibility gap, while the one with $T/T_c=0.95$ is outside, though still below the critical temperature.

III. MEASURING PRECIPITATE SIZES

We used two different measures of the sizes of the precipitates. One, denoted by R, is the first zero of the pair correlation function. It corresponds to a picture in which the precipitates are thought of as fluctuations in the density of minority atoms. The second measure corresponds to a picture in which the precipitates are thought of as large clusters of minority atoms connected by nearest-neighbor bonds, surrounded by a matrix of the majority phase. The constitution of the matrix also includes clusters of minority atoms, but nearly all of these are much smaller. The total number of l-atom clusters, which we shall denote by n_l, is the sum of a contribution from the precipitates and from the matrix,

$$n_l=n_l^P+n_l^M, \tag{5}$$

and the average size of the precipitate clusters,

$$\langle l\rangle=\sum_l ln_l^P/\sum_l n_l^P, \tag{6}$$

then provides our second measure of the size of the precipitates.

This definition of $\langle l\rangle$ requires a knowledge of n_l^M, the distribution of clusters in the matrix. To obtain this, we made the assumption that the distribution of these clusters is the same as it would be at thermal equilibrium with the same concentration of monomers (clusters with $l=1$). If this concentration were very small, we could obtain the equilibrium concentration $c_l^{\rm eq}$ of clusters of l minority atoms from the formula[14]

$$c_l^{\rm eq}\approx Q_l c_1^l. \tag{7}$$

Here Q_l is the ''cluster partition function'' defined by

$$Q_l=\sum_{K:\#(K)=l} e^{-E(K)/kT}, \tag{8}$$

where the sum goes over all translationally inequivalent l-particle clusters K and the symbol $\#(K)$ means the number of sites in cluster K. Some of the Q_l (for $l\leqslant 10$) have been calculated for nearest-neighbor interactions by Sykes.[15]

Unfortunately, the concentrations in our simulation are not small enough for Eq. (7) to be accurate. A better approximation than Eq. (7) is given by the semiempirical formula[14]

$$c_l^{\rm eq}=Q_l c_1^l(1-\rho)^{2-2l}\quad (l\geqslant 2), \tag{9}$$

where $\rho=\Sigma lc_l$ is the overall density of minority atoms. A similar approximation for the simple cubic lattice, namely, $c_l^{\rm eq}=Q_l c_1^l(1-\rho)^{4-3l}$ $(l\geqslant 2)$, has been found[14] to agree quite well with computer simulations for $2\leqslant l\leqslant 10$ at temperatures $0.59T_c$, $0.81T_c$, and $0.89T_c$ and minority atom concentrations 0.015, 0.075, and 0.127, respectively. We compared Eq. (9) with the simulation data at different temperatures, and found that for cluster sizes $\leqslant 10$ the discrepancy was typically below 10%. There were only two cases where this approximation deviated from the data. First, for the thermal equilibrium at $0.95T_c$ (just outside the miscibility gap) the matrix contained at significant number of clusters larger than ten atoms, and since we used Eq. (9) only for $l\leqslant 10$, the part of the distribution with larger precipitates was not accounted for. The second case was the times immediately after the temperature change. In this case, the distribution of very small clusters was too far from equilibrium. These data points were discarded for further analysis.

To use Eq. (6), we calculated n_l^M from Eq. (9) in the form

$$n_l^M(t)=\begin{cases}[N(1-\rho)^2]^{1-l}Q_l[n_1(t)]^l & (l\leqslant 10),\\ 0 & (l>10),\end{cases} \tag{10}$$

where N is the total number of lattice sites, and we then obtained n_l^P from Eq. (5).

To check whether the definition of l contained in Eqs. (6) and (10) does provide a reasonable measure of the average precipitate size, we have plotted the corresponding linear dimension $\langle l\rangle^{1/2}$ against our other measure of precipitate size, R, during the phase separation process that follows a quench from infinite temperature (Fig. 1) to a temperature below T_c. In agreement with our expectations from dynamical scaling[16,17] the approximate relation $R=1.4\langle l\rangle^{1/2}$ holds at all

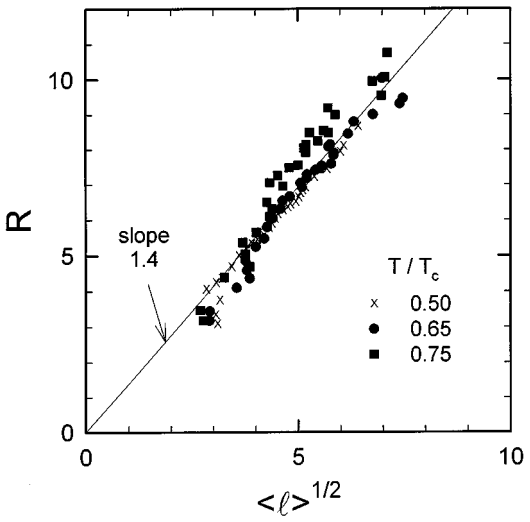

FIG. 1. The first zero of the correlation function R plotted against the average linear dimension of the clusters $\langle l\rangle^{1/2}$ at temperatures $T/T_c=0.5$, 0.65, and 0.75 after a quench from infinite temperature. The solid line is a linear regression to the entire data set.

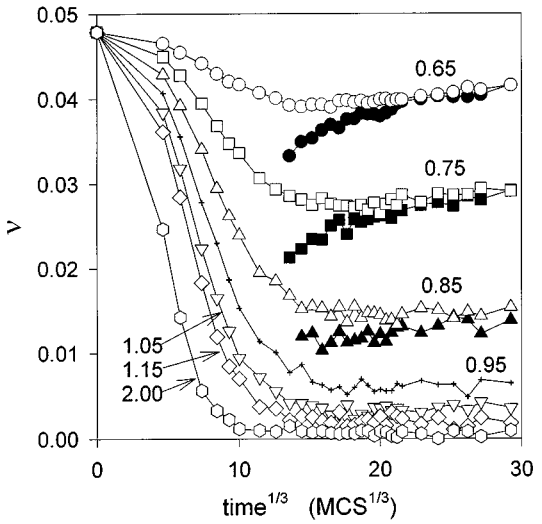

FIG. 3. More detailed view of the fraction of B atoms in large clusters. The solid symbols describe the evolution after quench from infinite temperature (growth and coarsening of precipitates). Open symbols (and plusses for $T/T_c=0.95$) show the process which occurs with a starting configuration prepared at $T/T_c=0.5$.

the times and all the temperatures considered, which supports our interpretation that $\langle l\rangle$ is a reasonable representation of precipitate volume.

IV. RESULTS

The results of the dissolution experiments, for various final temperatures, are shown in Figs. 2 and 3. For the first temperature in Fig. 2, $T/T_c=0.65$, the new phase point is still inside the misciblity gap of the phase diagram (Fig. 5); for the second, $T/T_c=0.95$, the phase point is outside the misciblity gap but is still below the line $T=T_c$; for the third, $T/T_c=1.15$, T is above the critical temperature.

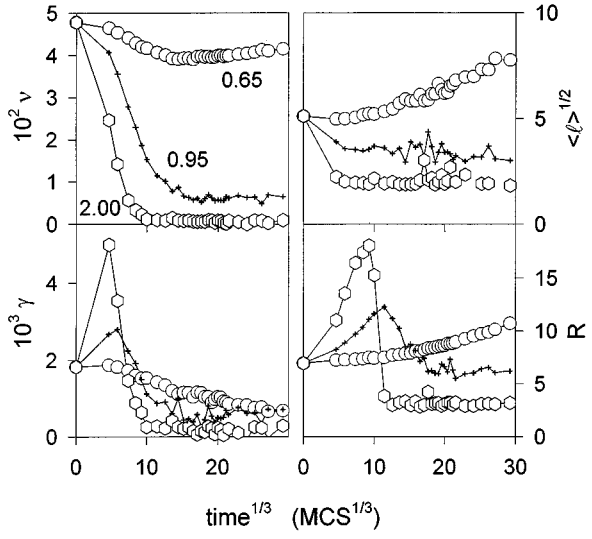

FIG. 2. Time dependence of various quantities during the dissolution of precipitates formed at the temperature $T/T_c=0.5$, after a jump to a higher temperature, $T/T_c=0.65$ (open circles), 0.95 (plusses), and 2.0 (open hexagons). The quantities plotted are the fraction ν of B atoms that are in large clusters (top left), the concentration γ of large clusters (bottom left), the square root of the average cluster size $\langle l\rangle=\nu/\gamma$ (top right), and R, the smallest zero of the pair correlation function (bottom right). The solid lines are guides to the eye.

The top left-hand diagram in Fig. 2 and also the more detailed diagram Fig. 3 show the time evolution of the fraction of atoms that are in precipitates, defined as

$$\nu=\sum_l ln_l^P/N. \tag{11}$$

During the first 10^4 or so MCS after the temperature jump, ν decreases to a value quite close to its equilibrium value as predicted by the lever rule. This is visible in Fig. 3 where at the temperatures $0.65T_c$, $0.75T_c$, and $0.85T_c$ different initial conditions lead to the same values of ν after a time in the order of 10^4 MCS. Immediately after the temperature jump the average cluster size, as measured by $\langle l\rangle$, also decreases, though the decrease is hardly noticeable if the final phase point is inside the miscibility gap (see Fig. 2, top right). If the new phase point is inside the miscibility gap, then $\langle l\rangle$ eventually begins to increase again; if it is outside, then $\langle l\rangle$ does not change any more, apart from fluctuations.

Surprisingly, the behavior of our other measure of precipitate size, the first zero of the pair correlation function (Fig. 2, bottom right), is quite different from that of $\langle l\rangle^{1/2}$. If after the temperature jump the phase point is still inside the miscibility gap (e.g., $T/T_c=0.65$), R increases slowly but steadily. If the temperature jump takes the phase point outside the miscibility gap, the initial increase of R is more dramatic. If the final temperature is above T_c (see the case $T/T_c=2.0$ in Fig. 2), R rises rapidly to as much as 3 times its original value and then falls quickly, stabilizing at a very low value which seems to correspond to equilibrium at the final temperature, but if the final temperature is below T_c (case $T/T_c=0.95$ in Fig. 2), the peak in R is lower and the subsequent decay of R slower, lasting for at least 2000 MCS.

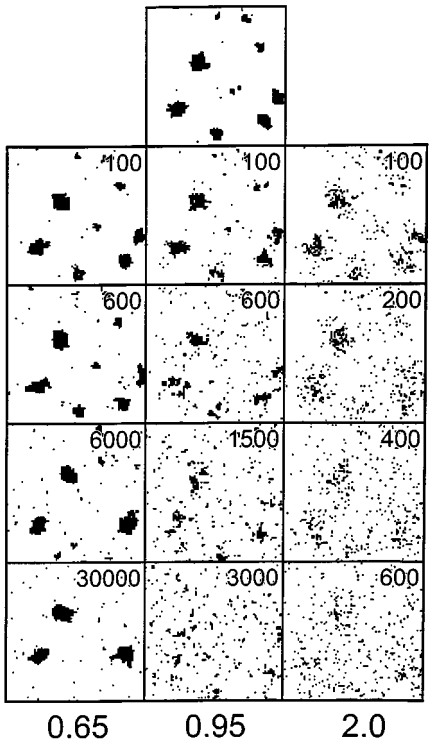

FIG. 4. Snapshot picture of the evolution of the model alloy at temperatures (a) $T/T_c=0.65$, (b) 0.95, and (c) 2.0. The initial configuration, obtained after 1000 MCS at $T/T_c=0.5$, is shown on the top. The numbers give the time in MCS starting from the initial configuration.

The behavior of the number of precipitates divided by the number of lattice sites, given by

$$\gamma=\sum_l n_l^P/N, \tag{12}$$

is shown in the bottom left-hand diagram of Fig. 2. This quantity is related to those in the top two diagrams by $\gamma=\nu/\langle l\rangle$. For temperatures well below T_c, it remains approximately constant during the first 1000 MCS, indicating that the temperature change does not create or destroy any precipitates; afterwards, γ decreases slowly, apparently because the smaller precipitates shrink and eventually disappear in a coarsening process. For the higher temperatures (outside the miscibility gap), there is an unexpected increase in the number of large clusters at first. This appears to be connected with the opposite behavior of R and $\langle l\rangle^{1/2}$: As the material in the precipitate spreads out, the large clusters tend to break up into two or even more large pieces which makes R increase and $\langle l\rangle^{1/2}$ decrease. Later on, γ falls to a value close to zero, as is to be expected if the precipitates dissolve.

The different regimes we have noted are also evident in the snapshot pictures of Fig. 4. For a final phase point inside the misciblity gap [case (a)], all the precipitates shrink at first and the small ones dissolve altogether, until the concentration in the matrix reaches its new (higher) equilibrium value. After this the largest clusters grow again by a slow coarsening process. Outside the misciblity gap, but below the critical temperature [case (b)], the precipitates shrink initially as in case (a), but now they all continue to shrink, remaining in a more or less compact form until they disappear altogether. In the third case, that of final temperatures above T_c [case (c)] the precipitates ''explode'' immediately into a large number of very small pieces, which stay close to each other for quite a long time. Each precipitate is replaced by a concentration fluctuation which then diffuses away slowly. The reason for the strong initial increase of R, unaccompanied by an increase of $\langle l\rangle$ (see Fig. 2) , is that R measures the size of these large-scale concentration fluctuations, whereas $\langle l\rangle$ decreases because it measures the sizes of the small connected pieces into which the original cluster has broken. Later on, as the correlated regions become larger, the density in them decreases; eventually they are no longer distinguishable from normal fluctuations and R drops back to a normal value.

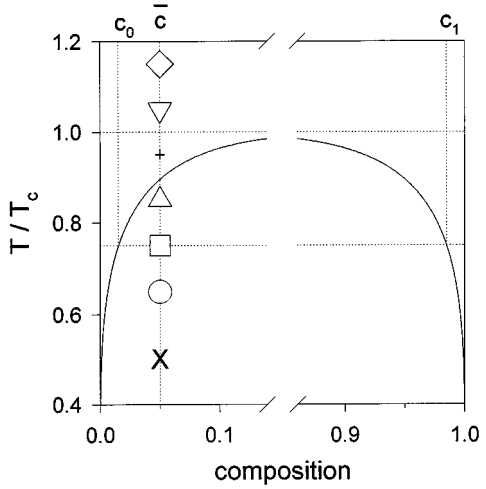

FIG. 5. The phase diagram of the Ising model on the square lattice. The solid line is the Yang formula [Eq. (4)]. The symbols show the phase points where computer experiments were performed.

V. A THEORETICAL MODEL

We use a phase-field kinetic model which treats the local concentration of B atoms as a function of space and time, $u(\mathbf{r},t)$, say, which is continuous except at the phase boundaries. At a phase boundary, if we neglect the effect of boundary curvature, u takes the value $c(T)$ on one side and $1-c(T)$ on the other, where $c(T)$ and $1-c(T)$ are the concentrations of B atoms of the two phases in equilibrium at temperature T. The functions $c(T)$ and $1-c(T)$ are shown graphically on the phase diagram, Fig. 5, and some possible profiles of u near a precipitate are shown in Fig. 6.

In the following we give a qualitative theoretical picture of the dissolution process, in three dimensions so that the model can be compared with experimental data. A simple way to relate u to our measure $\langle l\rangle$ of cluster size is to assume that in the regions where u is less than the percolation density[18] there are no large clusters, but that in regions where u is greater than this value a certain fraction of the particles (depending on the density) form a large cluster, this fraction being the same as it would be for an infinite system at that density. Since our main interest here is in qualitative behavior, we take the fraction of large clusters to be zero in the region where $u<\frac{1}{2}$, whereas if $u>\frac{1}{2}$, we assume that all the

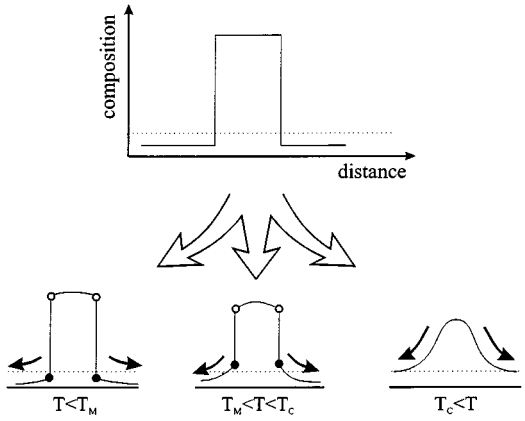

FIG. 6. Schematics of the dissolution process of precipitates after a jump to higher temperatures. The dotted line indicates the average composition ρ of the alloy, and the open and solid circles the equilibrium compositions of precipitates and matrix, respectively, at the temperature T.

particles present are in large clusters. Thus $\langle l\rangle$ is equal to the integral of u over the region where it is greater than $\frac{1}{2}$. We shall assume further that the regions where $u>\frac{1}{2}$ are spheres, all having the same radius a (which may depend on time), and that the value of u inside each sphere is uniformly $1-c(T)$. Then the above recipe for $\langle l\rangle$ gives

$$\langle l\rangle=[1-c(T)]\frac{4\pi a^3}{3}. \tag{13}$$

To relate u to R, we think of the sytem as consisting of a matrix where the density of B atoms is uniform together with identical precipitates centered at points $\mathbf{r}_1,\mathbf{r}_2\ldots$ so that u can be written

$$u(\mathbf{r},t)=c_0(t)+\sum_i u_0(\mathbf{r}-\mathbf{r}_i,t), \tag{14}$$

where $c_0(t)$ is independent of position and $u_0(\mathbf{r},t)$ is the local density of B atoms for a single cluster centered at the origin. The pair correlation function, defined as the space average (with respect to $\mathbf{r}'$) of $[u(\mathbf{r}',t)-\overline{u}][u(\mathbf{r}+\mathbf{r}',t)-\overline{u}]$ where $\overline{u}$ is the space average of $u(\mathbf{r},t)$, is then the convolution of the pair correlation function g for the points $\mathbf{r}_1,\mathbf{r}_2,\ldots$ with $u_0(\mathbf{r})*u_0(-\mathbf{r})$, where the asterisk denotes a convolution. A simple approximation for g is[19]

$$g(\mathbf{r})=\begin{cases}\gamma\delta(\mathbf{r})-\gamma^2 & (r<b),\\ 0 & (r>b),\end{cases} \tag{15}$$

where γ is the number of clusters per site and b is the radius defined by

$$\gamma\frac{4\pi b^3}{3}=1, \tag{16}$$

so that the space average of g is zero. If the range of $u_0(\mathbf{r})*u_0(-\mathbf{r})$ is less than $\frac{1}{2}b$, then Eq. (15) gives (for $r<\frac{1}{2}b$)

$$g(\mathbf{r})*u_0(\mathbf{r})*u_0(-\mathbf{r})=\gamma u_0(\mathbf{r})*u_0(-\mathbf{r})-\gamma^2\left(\int u d^3\mathbf{r}\right)^2, \tag{17}$$

and so, if $R<\frac{1}{2}b$, it is the smallest value where the average of $u_0(\mathbf{r})*u_0(-\mathbf{r})$ over the sphere $|\mathbf{r}|=R$ is equal to $\gamma(\int u d^3\mathbf{r})^2$. For example, if u_0 is a constant inside a sphere of radius a and zero outside, and $a<b/4$, then R is a little less than $2a$, becoming equal to $2a$ when γ is very small.

We use the sharp interface approximation to treat the problem and we also neglect the boundary curvature. According to this approximation, the value of u_0 jumps from $1-c(T)$ inside to $c(T)$ outside. Away from the interface u is a continuous function of the position vector $\mathbf{r}$ and obeys the diffusion equation. The velocity of the interface in the direction of its own normal is given by

$$V=-D[\partial u_0/\partial n]/[u_0], \tag{18}$$

where D is the diffusivity of B atoms relative to a background of A atoms, $[u_0]$ or $[\partial u_0/\partial n]$ denotes the discontinuity in u_0 or $\partial u_0/\partial n$ across the interface, and $\partial u_0/\partial n$ is the directional derivative of u_0 along the normal direction.

We denote the temperature just before the temperature jump by T_0 so that the equilibrium concentration of B atoms in the A-rich phase is then $c(T_0)$. Each precipitate will be approximated as a spherical region. Taking the origin of space at the center of a precipitate whose radius is a, and the origin of time at the moment when the temperature is increased, we have

$$u_0(r,0)=\begin{cases}1-c(T_0) & (r<a),\\ c(T_0) & (r>a)\end{cases} \tag{19}$$

(see Fig. 6, top). This formula gives the initial condition for the subsequent time evolution, but this takes place at a different temperature, so that the values of u_0 near $r=a$ change immediately.

Consider first the case where the new temperature, T, say, is less than the critical temperature T_c. The interface survives the jump, but the new values of u_0 on the two sides will be closer together than before. Calling $a(t)$ the radius at time t, the evolution of a will be governed by

$$da/dt=-D[\partial u_0/\partial r]/[1-2c(T)], \tag{20}$$

where

$$u_0(a(t)-0,t)=1-c(T),\quad u_0(a(t)+0,t)=c(T),$$

with $c(T)$ greater than $c(T_0)$, though still less than $\frac{1}{2}$. Initially the gradient of u_0 is the same on both sides of the interface, so that $da/dt=0$: The interface does not move. Here B particles are lost from the cluster by diffusion but, initially at least, its radius does not change. Indeed, since B particles move away from the center of the cluster, we may expect the pair correlation function for B atoms to become more spread out in space, so that the position of its first zero, which is our measure R of size, will increase initially. On the other hand, $\langle l\rangle^{1/2}$ decreases initially because particles are lost from the cluster. This initial behavior for R and $\langle l\rangle^{1/2}$ can be seen in Fig. 2.

As time proceeds, the initial antisymmetry of $c-\frac{1}{2}$ about the interface will be lost. The gradient of u_0 just inside the the interface will begin to be affected by the condition that the gradient has to be zero at $r=0$, and so the gradient will be closer to zero just inside the phase boundary than just outside, and the interface will move inwards. Soon a long-lived regime will be reached in which the time derivatives in the diffusion equation (though not in the equation for the velocity of the interface) can be neglected.[20] The concentration field near a precipitate is then given by

$$u_0=1-c(T) \quad [r<a(t)],$$
$$u_0=\phi(r) \quad [r>a(t)], \tag{21}$$

where ϕ is the solution of Laplace's equation which equals $1-c(T)$ for $r=a$ and satisfies the additional condition that the overall concentration of B atoms is ρ. Equations (20) and (21) may be solved to estimate the time dependence of the precipitate radius a (see the Appendix):

$$a\frac{da}{dt}=K(a)[\rho-c(T)-Ma^3], \tag{22}$$

where K and M are positive quantities defined in the Appendix, M being independent of a. Equation (22) shows that a will decrease until either a or the right-hand side of the equation becomes zero. Which of these two happens depends on the final temperature. If the final phase point is inside the miscibility gap, then $\rho-c(T)$ is positive and there is a positive value of $a^3\propto\langle l\rangle$ [see Eq. (13)] that makes the right-hand side of the equation zero. In the simplified treatment given here, $\langle l\rangle$ remains at this value forever, but in practice it will now increase slowly because of coarsening, which depends on an effect we have ignored, namely, the curvature dependence of the values of u at the interface.

If the final phase point is outside the miscibility gap, however, $\rho-c(T)$ is negative and so the right-hand side of Eq. (22) is always negative: The mean cluster radius a decreases until the clusters disappear altogether.

Finally, we consider the case where the final temperature is above the critical temperature. In this case there is no interface after the temperature jump; to find out what happens to a precipitate we use the diffusion equation

$$\partial u_0/\partial t=D\nabla^2 u_0, \tag{23}$$

with initial condition (19) and the boundary condition $\partial u_0/\partial r=0$ for $r=b$. As a rough estimate of R, the first zero of the pair correlation function, we use the mean square radius of the precipitate. According to Eq. (23) we have

$$\frac{d}{dt}\int u_0 d^3\mathbf{r}=\int D\nabla^2 u_0 d^3\mathbf{r}=0,$$
$$\frac{d}{dt}\int r^2 u_0 d^3\mathbf{r}=\int Dr^2\nabla^2 u_0 d^3\mathbf{r} \tag{24}$$
$$=6D\int u_0 d^3 r-4\pi Db^2 u_0(b,t),$$

so that the mean square radius increases linearly with time until $u_0(b,t)$ becomes appreciable. Thus we expect R^2 also to increase linearly with time until the expanded precipitates merge into one another, that is, until $R\sim b$. After this time the approximation of R by the mean square radius is no longer valid. The obervations do indeed show R increasing rapidly with time, falling back later on to a value close to what it would be if there were no precipitates. On the other hand, the average cluster size $\langle l\rangle\propto a^3$ decreases almost immediately to a low value because the expansion of the precipitate soon reduces the local density to a value where large clusters are very unlikely.

VI. DISCUSSION

Our interpretations of the observed precipitate dissolution process are illustrated in Fig. 6 which shows the spatial variation of u under various conditions. The solid circles represent values of $c(T)$, the equilibrium concentration of B atoms in the matrix at the new temperature, and the open circles represent values of $1-c(T)$, the equilibrium concentration of B atoms in the precipitates. The dotted line represents ρ, the overall concentration of B atoms. The height of the curve at the edge of the diagram corresponds approximately to the composition of the matrix. The left side of Fig. 6 shows the case where the final phase point is inside the miscibility gap. Since the solid circle in this figure is below the average composition of the whole alloy, the dissolution of some of the clusters will eventually lead to a sufficient increase in matrix concentration to stop the shrinking of the precipitates and allow some of them to grow again. Before this can happen, $\langle l\rangle$ has to decrease in order to allow the concentration in the matrix to increase to its equilibrium value.

The case where the new phase point is outside the miscibility gap but the temperature is still below T_c is illustrated in the middle of Fig. 6. Since the solid circle is *above* the dotted line, symbolizing the average composition of the alloy, the equilibrium level can never be reached and all the precipitates have to dissolve eventually.

A very similar picture has been used by Okuda *et al.*[5,7] to explain the observed increase of R in the case of the dissolution of precipitates in Al-Zn. In the alloy Al-Li, however, no increase of R was found.[6] This latter effect might be due to the fact that the precipitates in Al-Li consist of the ordered intermetallic phase Al_3Li, and ordering was not taken into account in the present simulations. Moreover, the simulations show that, for the case $T_M<T<T_c$, the increase of R is followed by a gradual decrease (see Fig. 2) in which the concentration shell around the dissolving precipitate shrinks by diffusion at the same time as the precipitate itself. Possibly, the experimental data for Al-Li might also be connected with this phenomenon.

The most spectacular effect occurs when the final temperature is above T_c. In this case, the density of the precipitate can decrease freely, the only limitation being diffusion (see Fig. 6, right). This leads to a rapid disintegration (or ''explosion'') of the precipitate and the formation of a concentration fluctuation that increases in size and decreases in density, in agreement with the observations in Fig. 4.

Our reason for using vacancy dynamics in these simulations, rather than the more common Kawasaki dynamics, was that in most alloys the vacancy mechanism is much

more important than the exchange mechanism.[21] However, if we had used Kawasaki (exchange) dynamics instead, we believe that the results would have been essentially the same, since in other types of simulation vacancy and Kawasaki dynamics do not give very different results until the temperature is below about half the critical temperature.[11]

ACKNOWLEDGMENTS

This work was supported in part by the FWF (Project No. S5601). We thank O. Paris, G. Vogl, and R. Weinkamer for discussions.

APPENDIX

To get an estimate for the time dependence of the mean precipitate radius a, we start by computing the function $\phi(r)$ under the condition that the overall concentration of B atoms is ρ. We require that the average number of B atoms in a sphere of volume $1/\gamma$, where γ is the number of precipitates per site, should be ρ/γ (see sketch in Fig. 7). In three dimensions this condition gives $\phi=\mathcal{A}/r+\mathcal{B}$ where

$$c(T)=\mathcal{A}/a+\mathcal{B},$$

$$\rho/\gamma=[1-c(T)]\frac{4\pi a^3}{3}+\int_a^b\left(\frac{\mathcal{A}}{r}+\mathcal{B}\right)4\pi r^2 dr, \quad \text{(A1)}$$

with a and b defined by Eqs. (13) and (16). Solving for $\mathcal{A}$ we find

$$\mathcal{A}=-2a\frac{[\rho-c(T)]b^3-[1-2c(T)]a^3}{(b-a)(2b^2-ab-a^2)}. \quad \text{(A2)}$$

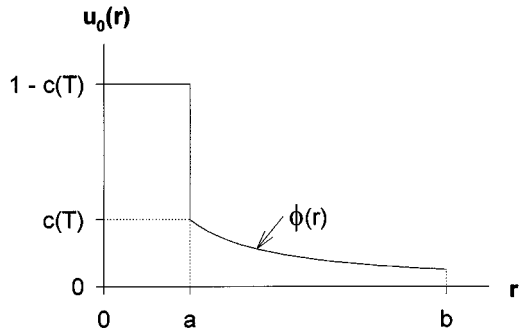

FIG. 7. Sketch of the local density $u_0(r)$ for a single precipitate centered at $r=0$. The integral of $4\pi r^2 u_0(r)$ between 0 and b is supposed fixed and equal to ρ/γ [see Eq. (25)] and $\phi(r)$ is a solution of Laplace's equation [see Eq. (21)].

The changing size of the precipitate can then be calculated by substituting Eq. (A2) into Eq. (21) and then Eq. (20), to get an equation which after multiplication by a reads

$$a\frac{da}{dt}=-\frac{D\mathcal{A}}{a[1-2c(T)]}=K(a)[\rho-c(T)-Ma^3], \quad \text{(A3)}$$

where

$$K(a)=2D/\{\tfrac{4}{3}\pi\gamma(b-a)(2b^2-ba-a^2)[1-2c(T)]\},$$

$$M=\tfrac{4}{3}\pi\gamma[1-2c(T)]. \quad \text{(A4)}$$

*Permanent address: Department of Mathematics, Heriot-Watt University, Riccarton, Edinburgh EH14 4AS, United Kingdom.

[1] For an overwiew of the theory of phase transitions see, e.g., J.D. Gunton, M. San Miguel, and P.S. Sahni, in *Phase Transitions and Critical Phenomena*, edited by C. Domb and J.L. Lebowitz (Academic, New York, 1983), Vol. 8; K. Binder, in *Materials Science and Technology*, edited by P. Haasen (VCH Verlagsges., Weinheim, 1991), Vol. 5, Chap. 7, p. 405.

[2] For an overwiew of experiments see, e.g., R. Wagner and R. Kampmann, in *Materials Science and Technology*, edited by P. Haasen (VCH Verlagsges., Weinheim, 1991), Vol. 5, Chap. 4, p. 213.

[3] D. Allen, S. Messoloras, R.J. Stewart, and G. Kostorz, J. Appl. Crystallogr. **11**, 578 (1978)

[4] K. Gerstenberg and V. Gerold, Cryst. Res. Technol. **20**, 79 (1985).

[5] H. Okuda, K. Osamura, H. Hashizume, and Y. Amemiya, Acta Metall. **36**, 899 (1988).

[6] H. Okuda, M. Tanaka, K. Osamura, and Y. Amemiya, Acta Metall. Mater. **41**, 1733 (1993).

[7] H. Okuda, M. Tanaka, K. Osamura, and Y. Amemiya, Scr. Metall. Mater. **27**, 1425 (1992).

[8] N. Nojiri and M. Enomoto, Scr. Metall. Mater. **32**, 787 (1995).

[9] A.B. Bortz, M.H. Kalos, J.L. Lebowitz, and M.A. Zendejas, Phys. Rev. B **10**, 535 (1974); J. Marro, A.B. Bortz, M.H. Kalos, and J.L. Lebowitz, *ibid.* **12**, 2000 (1975); M. Rao, M.H. Kalos, J.L. Lebowitz, and J. Marro, *ibid.* **13**, 4328 (1976); A. Sur, J.L. Lebowitz, J. Marro, and M.H. Kalos, *ibid.* **15**, 3014 (1977).

[10] K. Binder and D.W. Heermann, *Monte Carlo Simulation in Statistical Physics* (Springer, Berlin, 1988).

[11] P. Fratzl and O. Penrose, Phys. Rev. B **50**, 3477 (1994); C. Frontera, E. Vives, T. Castán, and A. Planes, *ibid.* **53**, 2886 (1996); P. Fratzl and O. Penrose, *ibid.* **53**, 2890 (1996).

[12] L. Onsager, Phys. Rev. **65**, 117 (1944).

[13] C.N. Yang, Phys. Rev. **85**, 808 (1952).

[14] M. Kalos, J.L. Lebowitz, O. Penrose, and A. Sur, J. Stat. Phys. **18**, 39 (1978).

[15] M. Sykes (private communication).

[16] J. Marro, J.L. Lebowitz, and M.H. Kalos, Phys. Rev. Lett. **43**, 282 (1979); J.L. Lebowitz, J. Marro, and M.H. Kalos, Acta Metall. **30**, 297 (1982); P. Fratzl, J.L. Lebowitz, J. Marro, and M.H. Kalos, *ibid.* **31**, 1849 (1983); P. Fratzl and J.L. Lebowitz, *ibid.* **37**, 3245 (1989).

[17] P. Fratzl, J.L. Lebowitz, O. Penrose, and J. Amar, Phys. Rev. B **44**, 4794 (1991).

[18] D. Stauffer and A. Aharony, *Introduction to Percolation Theory*, 2nd ed. (Taylor & Francis, London, 1992).

[19] P. Rikvold and J.D. Gunton, Phys. Rev. Lett. **49**, 286 (1982).

[20] R. Pego, Proc. R. Soc. London Ser. A **422**, 261 (1989).

[21] G.E. Murch, in *Phase Transformation in Materials*, edited by P. Haasen, Vol. 5 of *Materials Science and Technology* (VCH, Weinheim, 1991), Chap. 2, p. 75.